arXiv:1612.04396v1 [cond-mat.mes-hall] 13 Dec 2016

Acoustic Edge Magnetoplasmons and Quantum Hall Effect

V.B.Shikin
Institute of Solid State Physics, Russian Academy of Sciences,
142432 Chernogolovka, Russia

Abstract

Discussed in the present study are details of the behavior of low-frequency "acoustic" (*ac*) modes in the spectrum of edge magnetoplasma oscillations in axially symmetric degenerate 2D electron systems where electron density distribution $n(\vec{r})$ behaves as $n(\vec{r} \to R) \to 0$ when r approaches the external radius R of the domain occupied by electrons. It is shown that finding the dependence of the spectrum of *ac*-modes on radial (l) and azimuthal (m) indices when both l and m are small requires axially symmetric solution of the relevant problem. The desires is achieved in the so-called elliptic approximation for electron density distribution $n(\vec{r})$. The obtained results are employed to interpret available data on the excitation of *ac*-modes in degenerate electron disks with smooth electron density profile placed in the magnetic field H normal to the disk plane. The performed analysis confirms reported detection of the soft *ac*-mode in the range of $H \gg H_{max}$ where H_{max} is the field at which the maximum of the $\omega^s_{lm}(H)$ curve is observed (here and below $\omega^s_{lm}(H)$ stands for the frequency of the soft *ac*-mode).

A strong interaction of the *ac*-modes with (*integer*)-channels inevitably arising near the boundaries of 2D electron systems with smooth electron density profile as the magnetic field is varied in the Quantum Hall Effect (QHE) regime is emphasized. Well-formed *integer*-stripes can suppress some acoustic modes which is actually observed in experiments.

PACS:

Introduction

The existence of special low-frequency modes (later called "acoustic") in the spectrum of edge magnetoplasma (edge magnetoplasmons, EMP) oscillations was predicted in Refs. [1, 2]. Generally, EMP-oscillations propagate along the boundary of a 2D charged system placed in the magnetic field H normal to its plane. The existence of "acoustic" (*ac*; $AEMP$) modes requires vanishing of the charge density $n(\vec{r})$ at the disk boundary. Special attention to the condition $n(r)_{|r=R} \to 0$ (here R is the 2D disk radius) in the studies of EMP is easily understood. A necessary component in the formulation of all classical problems involving edge plasma oscillation is the requirement of vanishing normal component of induced current at the sample boundary

$$j_n(r \to R) = 0. \tag{1}$$

The charge density $n(\vec{r})$ in Eq. (1) is assumed to be finite up to the boundary $\vec{r} = R$. However, if the boundary is "soft", i.e.

$$n(r)_{|r=R} \to 0 \tag{2}$$

(for example, in 2D systems with externally controlled structure), Eq. (1) is satisfied automatically which should have a profound effect on the spectrum in such systems.

Calculations of the details of classical EMP spectrum in the system with "elliptic" density profile (the term "elliptic" is explained below, see Ref. [2] and Eq. (7)) confirms this guess. For a disk with finite radius R, in addition to the discrete plasmon spectrum modified by the cyclotron splitting due to magnetic filed H, a new acoustic mode arises whose frequency raises from zero at zero H (hence the term "acoustic") to some peak value at a certain H where

$$\partial\omega_{ac}(H = H_{max})/\partial H = 0, \tag{3}$$

after which ω_{ac} decreases approximately as $1/H$. $AEMP$-excitations were discovered [3,4] in a disk of surface ions in liquid helium exactly at the stage of their frequency going through the maximum as a function of magnetic field H which substantially simplified their identification. Various attempts (listed in the recent published studies [5–7] on the ω_{ac} problem) to perform similar experiments in degenerate electron systems have not yet been successful.

In practice, the expected for the ω_{ac} frequency range reveals a set of modes whose frequency diminishes monotonously with growing magnetic field which is typical of all varieties of EMP. Actually, an essential argument in favor of the *ac*-nature of the excitations observed in Ref. [7] is the inequality

$$\frac{\omega_{ac}(q,j)}{\omega_{ac}(q,j+1)} > 1, \tag{4}$$

(here q is the wave number along the disk boundary, j is the discrete index from the definition of $\omega_{ac}(q,j)$ (5)) which should be satisfied by *ac*-modes with different indices. Usually, the discrete EMP-excitations have the energy which increases with the growth of the azimuthal and radial indices. $AEMP$ modes behave in quite the opposite way as indicated by Eq. (4).

Inequality (4) is present in all versions [1, 2, 4, 8] of the *ac*-modes description. The solution [8] for the half-plane with the boundary where density profile $n(x)$ becomes zero: $n(x)_{|x\to 0} \to 0$ reveals this point in the most prominent way. A special choice of the density profile $n(x)$ in the half-plane problem allows to obtain an analytic expression for the spectrum of *ac*-modes

$$\omega_j(q) = -s_j q, \quad s_j = \frac{2\bar{n}_s e^2}{\epsilon m_e \omega_c j}, \quad j = 1, 2, 3... \tag{5}$$

Here ϵ is the effective dielectric constant, m_e is the effective mass, ω_c is the cyclotron frequency, $\bar{n}_s$ is the average density of the 2D system far from the transition domain, q is the wave number along the "soft" boundary. In the representation (5) $\omega_j(q)$ reveals no peaks monotonously decreasing with the magnetic field H, thus indicating that Eq. (5) is only applicable for sufficiently high fields exceeding the field at which the "acoustic" peak occurs. However, the dependence $s_j \propto j^{-1}$ which is typical of the *ac*-modes and, consequently, validity of the observed inequality (4) is present in the results of Ref. [8].

Observation of the property (4) derived from Eq. (5) is assumed to be sufficient proof of the "acoustic" nature of experimentally detected excitations. However, the results of Ref. [9] cast a doubt on this confidence. Here the $Hall-bar$-geometry and *time resolved* techniques were employed to detect the excitations whose velocities also comply with Eq. (5). The authors of Ref. [9] believe their measurements to be relevant to predictions of Ref. [8]. However, in the cell geometry used in Ref. [9] the requirement (2), which is a necessary condition for the existence of *ac*-modes (for details, see below), cannot be satisfied. In this connection, additional arguments [7] (mainly experimental) allowing to assume the existence of a smooth density profile possessing special properties (2) become important.

The point is that as the magnetic field approaches the range of $H \geq H_{max}$, the classical regime (5) changes to the threshold suppression of *ac*-modes in the fields approximately corresponding to integer filling factors $\nu_l = integer \quad (\nu = \pi l_{H_l}^2 \bar{n}_s, \quad l_H^2 = 2c\hbar/eH\ )$ within the homogeneous part of the 2D system at the disk center [5-7]. This the way the acoustic modes $\omega_{ac}^j(H)$ respond to the QHE state of the 2D system. In the present paper general arguments of Ref. [7] concerning possible reasons of strong influence of the QHE on *ac*-modes are filled with specific contents allowing to understand the details of observed transformation of *ac*-modes. This part of the study is based on modification of

the classical formalism [1, 2, 4, 8] employing the simplest possible approach to description of inhomogeneous systems, namely, local Drude approximation. The limits of this model by today's standards was discussed in detail in Refs. [10, 11] for Ohmic transport $\sigma_{ik}^{\parallel}(x)$ in the direction normal to the electron density gradient. Modification of the conduction properties $\sigma_{ik}^{\perp}(x)$ of inhomogeneous 2D system along the direction of dn/dx proves to be equally important. Details of this modification are directly related to the properties of *ac*-modes in the QHE regime, as shown in the present paper.

1. Classical EMP-excitations in the disk with elliptic density profile

A. In order to present a review of available results we first consider the main criteria (4), (5) of "acoustic" nature of the modes observed in Ref. [7] in axially symmetric terms. Any "flat" statement for edge excitations (including inequality (4)) is only meaningful for cylindrical geometry in the limit

$$\lambda \ll R, \tag{6}$$

where λ is the edge excitation wavelength, R is the characteristic radius of the studied disk. The relation given by Eq. (4) combined with Eq. (5) does not depend on q at all, suggesting either its universal nature with respect to requirement (6) or (which is more probable) its quantitative unsuitability in axially symmetric problems. The only possibility to find out the real state of things arises if an appropriate axially symmetric solution is available. In the present case this possibility is provided [2] by the known solution for the EMP-excitations in the disk with the elliptic density profile defined as

$$n(r) = n(0)\sqrt{(1 - r^2/R^2)}, \tag{7}$$

which is a suitable alternative to the profiles $n(x)$ employed in Refs. [1, 8].

The classical spectrum $\omega(l, m, \omega_c)$ of EMP-excitations in the disk with the density profile (7) and dissipationless tensor $\sigma_{ik}(r, \omega) = \sigma_{ik}(\omega)n(r)/n(0)$ within the Drude approximation

$$\sigma_{xx}(\omega) = \frac{i\omega n(0)e^2}{m_e(\omega^2 - \omega_c^2)}, \quad \sigma_{xy}(\omega) = \frac{\omega_c n(0)e^2}{m_e(\omega^2 - \omega_c^2)}, \quad \omega_c = \frac{eH}{m_e c} \tag{8}$$

($n(r)$ from (7), m_e is the free electron mass, c is the speed of light) normalized according to Ref. [2]

$$\Omega_{lm} = \Omega_0 / L_{lm}^{1/2}, \quad L_{lm} = 2\frac{\Gamma(l+m+1)}{\Gamma(l+m+\frac{1}{2})}\frac{\Gamma(l+1)}{\Gamma(l+\frac{1}{2})}, \quad \Omega_0^2 = \frac{2\pi n(0)e^2}{\varepsilon m_{\rm e} R}, \tag{9}$$

(ε is the ambient media dielectric constant, $\Gamma(x)$ is the gamma-function) has the following structure:

$$\omega_{lm}^2 - [\omega_c^2 + (2l+m)(2l+m+1) - m^2] = m(\omega_c/\omega_{lm}). \tag{10}$$

Here l, m are the radial and azimuthal indices taking any integer values starting from zero. To stress the difference between spectra (5) and (10), radial index in (10) is denoted by symbol l.

For $m > 0$ (the case of $m = 0$ means zero wave numbers and therefore is irrelevant) the follwing two parts of the dispersion equation (10) are of interest: the versions with $l = 0$ and $l > 0$. For $l = 0$ one of the roots of Eq. (10) coincides (to within its sign) with the cyclotron frequency $\omega_{0m} = -\omega_c$. This root should be ignored since when deriving Eq. (10) the original dispersion equation was multiplied by $(\omega^2 - \omega_c^2)$ [2]). the two remaining roots yield the frequencies (in usual units, s^{-1})

$$\omega_{0m}^{\pm} = \sqrt{\frac{|m|}{L_{0m}}\Omega_0^2 + \frac{\omega_c^2}{4}} \pm \frac{\omega_c}{2}, \quad L_{0m} = \frac{2}{\sqrt{\pi}}\frac{\Gamma(m+1)}{\Gamma(m+\frac{1}{2})}, \tag{11}$$

with Ω_0^2 from (9).

In the problem of ac - excitations the properties of clearly observed EMP modes (11) (shown in Fig. 1) are useful due to their adjusting possibilities employed below.

For $l > 0$, Eq. (10) is a cubic equation with respect to ω_{lm} and has three real roots correspnding to magnetoplasma oscillations of two types. First, there exist two modes whose frequencies $\omega_{lm}^{\pm}$ remain finite if $\omega_c \to 0$

$$\omega_{lm}^{\pm}(\omega_c \to 0) \to \Omega_0\sqrt{A_{lm}}/L_{lm}^{1/2}, \quad A_{lm} = [(m+2l)(m+2l+1) - m^2]. \tag{12}$$

In the limit $\omega_c \to \infty$ $\omega_{lm}^{\pm}$ asymptotically approach ω_c from above.

Second, there is a low-frequency ac-mode ($AEMP$) with the frequency first increasing with the growth of H as

$$\omega_{lm}^{s} \simeq m\omega_c/A_{lm}, \tag{13}$$

and then, passing through a peak (3), decreasing as ω_c^{-1}

$$\omega_{lm}^s \simeq \frac{\Omega_0^2}{\omega_c}\frac{m}{L_{lm}} \tag{14}$$

at $\omega_c \gg 1$ (dimensionless units (9)).

In the range of $l \gg 1$ the constants L_{lm} in (9) can approximately can be calculated as

$$L_{lm} \simeq 2\sqrt{l(l+m)}, \tag{15}$$

and therefore the limit of large l at fixed m in Eq. (14) yields

$$\omega_{lm}^s \simeq \frac{\pi n(0) e^2 m}{\varepsilon m_e \omega_c R\sqrt{l(l+m)}}. \tag{16}$$

Hence, for $l \gg m$ the asymptotic relations (5) and (16) both have the same structure: $j \leftrightarrow l$, and the relevant parameters are practically identical. Everything indicates a qualitative agreement between (5) and (16) in the limit (6).

As to the general case, Eq. (14) yields an axially symmetric alternative for the "flat" inequality (4)

$$\omega_{l,m}^s/\omega_{l,(m+1)}^s = \frac{mL_{l,m+1}}{(m+1)L_{l,m}} < 1, \quad \omega_{l,m}^s/\omega_{(l+1),m}^s = \frac{L_{l+1,m}}{L_{l,m}} > 1 \tag{17}$$

where $L_{l,m}$ is from (9).

B. Papers [5-7] do not contain description of the details of the mechanism used to excite different modes. Hence the only way to identify the indices actually governing the spectra is to analyze the behavior of the spectra themselves. One of stages of this analysis concerns the choice of index m. Let us consider the available data. Analysis of the upper right inset in Fig. 1 [7] reveals that in the j-representation the ratio of the frequencies $\omega_{j=1}^{exp}/\omega_{j=2}^{exp} \leq 1.9$ (approximately 1.8–2.0, the accuracy of this numeric interval is rather low) for not too high magnetic fields (where no signs of suppression are yet observed) and does not depend on m (i.e., on q) at all. In the l-representation given by Eq. (14) this observable ratio leads, according to (17), to the requirement (18) expressed as an equation for m

$$\frac{L_{lm}(l=2,m)}{L_{lm}(l=1,m)} \simeq 1.9. \tag{18}$$

Trying in Eq. (18) various possible small values of index m, one arrives at the following result: the case of $m = 0$ is irrelevant, $m = 1$ yields $L_{lm}(l = 2, 1)/L_{lm}(l = 1, 1) = 1.6$.

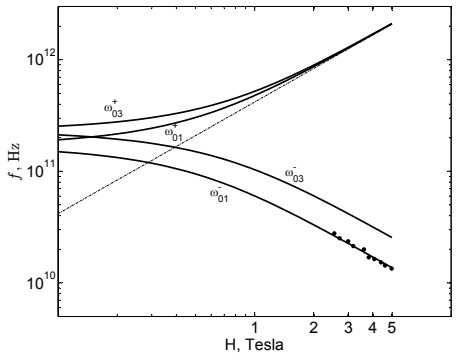

Figure 1: Magnetoplasmon frequencies (10), (11) with $m = 1$, $m = 3$, $l = 0$ for the disk with elliptic equilibrium electron density profile. Dashed line: $\omega = \omega_c$. The choice of $m = 1$ is described in the comments to Eq. (18), while index $m = 3$ just demonstrates the increase in the energy of the EMP-mode with growing indices (an alterative to Eq. (4), the frequency ω_{0m}^{-} increases with m). The rest numbers are given in the text in the comments to the figure. Shown in the lower branch are the experimental data for $\omega_{01}^{-}(H)$ from [5]. Adjustment was performed with the parameter $n(0)$ as described in the text.

The rest values $m > 1$ only reduce this ratio which tends to unit for large m. The index $m = 1$ provides the value closest to that given by Eq. (18). Not too impressive numerical agreement between 1.9 and 1.6 can be explained by non-ellipticity of real disks used in Refs. [5–7].

Frequencies $f = \omega/(2\pi)$ in units of s^{-1} of elliptic EMP-modes (10), (11) with indices $(l = 0, m = 1)$, $(l = 0, m = 3)$ and normalization (9) are presented in Fig. 1. The plots are drawn taking into account data of Figs. 1 and 2 from Ref. [5]: disk radius $R = 15$ μm, electron mass $m_e = 0.067 m_0$, effective dielectric constant of the ambient medium $\varepsilon = 6.9$. The field B is replaced with H since $\mu \simeq 1$, electron density at the disk center $n(0) = 6.3 \times 10^{11}$ cm^{-2} (used as adjustable parameter to fit the experimental frequencies [5] ignoring the density of 2.2×10^{11} cm^{-2} corresponding to the average sample density before etching). The relevant experimental points lie on the curve ω_{01}^{-} in the lower right part of the figure. The curve $(l = 0, m = 3)$ is plotted to demonstrate an increase in the energy of EMP-modes with growing indices (an alternative to Eq. (4)).

$AEMP$-part of the problem is represented numerically by plots in Fig. 2 where the indices $m = 1$, $l = 1$, are used combined with the normalization (9); the required numerical disk parameters are the same as those adopted for calculations of EMP-modes

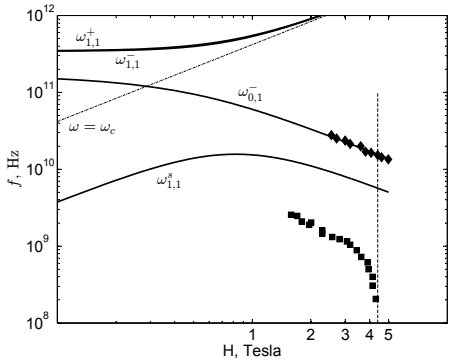

Figure 2: Magnetoplasmon spectrum ω_{lm} (10),(12) for $m = 1,\ l = 1$. Two upper curves corresponding to $\omega^{\pm}_{1,1}$ have a slight linear in H splitting at $H \to 0$ and the lower of them has a shallow minimum practically indiscernible in the figure. The lowest curve representing the $AEMP$-mode ω^{s}_{11} with the numbers identical to those of EMP-plots in Fig. 1 illustrates position of the $AEMP$-peak with respect to the range of magnetic fields studied in Ref. [7]. The experimental data for $AEMP$-modes [7] are shown by squares. Plotted for comparison is the curve $\omega^{-}_{01}(H)$ from Fig. 1 with experimental points (diamonds) used to normalize all the numbers in Figs. 1 and 2. Vertical dash-and-dot line indicates the threshold above which the $AEMP$-mode vanishes. The same line indicates that the EMP mode $\omega^{-}_{01}(H)$ is practically insensitive to the threshold.

plotted in Fig. 1. The upper part of Fig. 2 contains information on frequencies $f = \omega^{\pm}_{lm}/(2\pi)$ following from (10) and covering asymptotic behavior given by Eq. (12). The lower branch $f = \omega^{s}_{lm}/(2\pi)$ is drawn according to Eq. (10) for the mode with $l = 1, m = 1$ within the range of magnetic fields where the peak for ac-excitations can coexist on a single figure with the experimental points (black squares) reported in Fig. 1of Ref. [7].

In addition to the $AEMP$-part of the spectrum, Fig. 2 contains EMP-resonances $\omega^{-}_{01}(H)$ (black diamonds) also shown in Fig. 1. The purpose of this juxtaposition is to demonstrate the absence of visible signs of suppression of EMP modes at magnetic fields where the $AEMP$ excitations already no longer exist. The observed selectivity (some modes vanish while others persist) is characteristic of the mechanisms of the mode suppression discussed in section **2.**

A noticeable difference in Fig. 2 between the observed and calculated frequencies $f = \omega^{s}_{11}/(2\pi)$ obtained by fitting of the EMP-resonances $\omega^{-}_{01}(H)$ is somewhat disappointing. On the other hand, it is appropriate to remind the original reasons of turning to the axially symmetric formalism in the description of the $AEMP$ excitation against

the background of predictions [8] for the semi-infinite model of the 2D system. There were some arguments suggesting a qualitative difference in the structure of inequalities (4) and (17) that were actually confirmed later. A possibility arose for a thorough analysis of the azimuthal indices m whose values are actually determined by the details of the EMP-modes excitation technique. In the final results of Ref. [5] this index is a free parameter. A justification was developed for dealing with the frequencies themselves rather only their ratios. As a result, a qualitatively understandable picture presented in Fig. 2 was derived where the position of branches ω^s_{11}, ω^-_{01} relative to the line $\omega = \omega_c$ is shown and the peak location $H = H_{max}$ (3) is indicated. One can hardly hope for the elliptic model to claim for anything more. As to the indicated numerical discrepancy, it originates not only from the poor agreement of the density profile adopted in the elliptic model (7) and the real disks. The data of Ref. [5] for the EMP-part of spectrum reveal that changing the nominal disk size 4 times (from 5 to 20 mcm) only reduces the frequency of the ω^-_{01}-mode by a factor of 2 which is quite unexplainable within the traditional theory of EMP-excitations [20]. As a consequence this puzzle is also transferred to the $AEMP$-domain.

One more reason for numerical disagreement in frequencies is the deviation of the $\omega^s_{lm}(H)$ curve from the asymptotic law (14) in the entire range of experimentally studied magnetic fields [7], as shown in Fig. 2. In this domain the *ac*-modes start feeling their "'end" of quantum origin marked in Fig. 2 by a vertical line. Quantitative description of the $\omega^s_{lm}(H)$ behavior in the vicinity of the threshold is still missing. The origin of the threshold itself is discussed below in Section **2.**

2. Influence of integer stripes on the dynamics of *ac*-modes

A. Typical structures developing on the density profile $n(r)$ in the QHE regime are flat areas with $dn/dx = 0$ (integer channels) in the vicinity of points x_l where $\nu(x_l) = integer$

$$\nu(x) = \pi l^2_{H_l} n(x),, \quad l^2_H = 2c\hbar/eH \tag{19}$$

Chklovsky et al. [12, 13]). Fig. 3 depicts two such stripes located at the points where $\nu(x_2) = 2$ and $\nu(x_4) = 4$ that were calculated self-consistently in Refs. [14–16]. The left axis measures the local filling factor $\nu(x)$ from (19) for the electron density profile $n(x)$

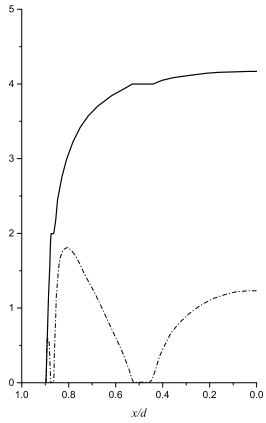

Figure 3: Filling factor $\nu(x)$ (solid line) containing flattened areas where $d\nu(x)/dx = 0$ (integer shelves, the origin of the term is explained below) and the profiles of the conductivity $\sigma_{xx}^{\perp}$ in the direction normal to the integer shelves axes (dash-and-dot line) for the left half of a symmetric sample with $d = 1.5\mu m$, $n_s = 4 \cdot 10^{11} cm^{-2}$, $b = 0.9d$ calculated within the $TFA - SCBA$ approximation (Thomas-Fermi approximation employing the self-consistent Born approximation) by authors of Ref. [16] (a part of Fig. 5 from [16]).

as a function of position x (solid line in the figure) and local value of $\sigma_{xx}^{\perp}(x)$ (dash-and-dot line) at the same points. The density profile $n(x)$ of a one-dimensional symmetrical $[n(x) = n(-x)]$ about the origin $x = 0$ two-dimensional system considered in Ref. [16] has clearly defined zeros at the system boundaries $[n(b) = n(-b) = 0]$. Position of movable zero points $\pm b$ relative to the sandwich boundaries $\pm d$ is controlled by external parameters described in detail in Refs. [14–16]. Fig. 3 is drawn for $d = 1.5\mu m$, $b = 0.9d$. When magnetic field normal to the plane of 2D system is gradually raised it finally reaches a threshold value H_{thresh} sufficient for development of as single (and for higher fields even multiple) integer shelf on the density profile. Shown in Fig. 3 are two such shelves. The first one corresponds to $\nu_l = 2$, while the second has $\nu_l = 4$. Even values of the filling factor are due to the particular approximation adopted in Ref. [16] (neglect of the electron spin).

The data of Fig. 3 allow to distinguish (as to EMP) between smooth and sharp transition domains in the electron density behavior. The profile $n(x)$ is considered to be smooth if the integer shelf width $2a_l$ at its slope is small compered with the length scale

of the transition domain of $n(x)$. Bearing in mind the definition of a_l from [12]

$$a_l^2 = 2\kappa\hbar\omega_c/(\pi^2 e^2 dn(x_l)/dx) \tag{20}$$

(κ is the ambient medium dielectric constant, ω_c is the cyclotron frequency) and the estimate for the transition domain width w as given by (21)

$$w \simeq \int_0^\infty dx[n_\infty - n(x)]/n_\infty, \tag{21}$$

one obtains the requirement for smooth profile in the form

$$a_l \ll w. \tag{22}$$

It should be noted that the very definition of a_l (20) has some limitations. The calculations performed assumed a possibility for arising electrostatic fields to vanish far from the central part of the shelf located at x_l. This simplification requires careful treatment of the shelf properties near the edges of 2D system [17], [18] (for Fig. 3, this is the shelf with $\nu = 2$).

Apart from confirming the hypothesis of the authors of Refs. [12, 13] concerning the possibility of formation of *integer* shelves, the papers of Gerhardts and coauthors [16] proposed a technique for calculation of the conductivity $\sigma_{xx}^{\perp}(x)$ under inhomogeneous conditions of Fig. 3. According to their calculations (dash-and-dot line in Fig. 3) the conductivity $\sigma_{xx}^{\perp}(x)$ becomes zero in the areas where $dn(x)/dx = 0$. This is most clearly seen for $\sigma_{xx}^{\perp}((x)$ within the shelf with $\nu_l = 4$.

Taking into account the importance of anomalous behavior of the conductivity $\sigma_{xx}^{\perp}(x)$ following from the calculations [16]

$$\sigma_{xx}^{\perp} \equiv \sigma_{xx}(\nu_l) \equiv 0, \tag{23}$$

(the conductivity of an *integer*-stripe in the direction normal to its axis is zero), it is useful to mention the direct experiments [19] favoring Eq. (23). Reported in the review [19] are data on the IVC of a single *integer*-stripe in the direction normal to its axis. It is shown that in the Ohmic range it is strongly non-linear in the sense that

$$\partial J/\partial V_{V\to 0} \to 0, \tag{24}$$

(J is the total current crossing the stripe, V is the potential difference at its sides), which is equivalent to the property $\sigma_{xx}^{\perp} \simeq 0$ (23).

B. According to Fig. 3, apart from the domain $n(r \to R) \to 0$ which is a necessary component of the classical theory of *ac*-modes [1, 2, 8] (based on the local Drude definition of the conductivity $\sigma_{xx} \propto n(x)$ covering the area where $n(r \to R) \to 0$), the QHE regime features additional domains with prominent modulation of the 2D system conductivity. In that case classical approximation $\sigma_{xx} \propto n(x)$ fails even qualitatively.

Quantitative analysis of the QHE-induced features in the behavior of *ac*-excitations due to development of *integer*-stripes on the density profile $n(x)$ can be performed in two ways: by directly including information of Fig. 3 for $\sigma_{xx}^{\perp}(x)$ into equations describing EMP dynamics; or (without claiming any numbers) approximately, by replacing the details in the behavior of $\sigma_{xx}^{\perp}(x)$ shown in Fig. 3 with the boundary conditions prohibiting charge transfer through the shelves.

Let the area $x = x_4$ be the sole *integer*-channel on the density profile $n(x)$ shown in Fig. 3. Then to the right of point x_4 (chosen as the origin) equilibrium electron density is almost uniform so that the set of equations for the oscillating part of $\delta n_s^{>}(x,t)$ has the standard structure typical of the EMP formalism [20]. The required solution $\varphi_{>}(x,y,t)$ should decay towards the sample center and satisfy the requirement

$$j_{\perp}(x \to +0) = 0. \tag{25}$$

In the vicinity of $x = 0$ electron density is not zero. Hence, condition (25) has the sense of requirement (1). The difference between (1) and (25) is that the potential $\varphi_{>}(x,y,t)$ from (1) to the right of point $x = 0$ is the only one relevant to the problem. Its involvement in the boundary condition (1) finally leads to the EMP dispersion law. The problem (25), in addition to the right part of the 2D system, there exists the left part between the point $x = x_4$ and the boundary of the system where electron density vanishes. The requirement (25) prevents the charge exchange between the left and right parts of the *integer*-stripe. However, the mutual influence of the fields $\varphi_{>}(x,y,t)$ and $\varphi_{<}(x,y,t)$ on the conducting areas to the left and to the right of the cut (see below) contributing to the spectrum formation remains finite.

The potential $\varphi_{>}(x,y,t)$ for the problem (25) (with the origin shifted to the center of the *integer*-stripe) is written as

$$\varphi_>(x,y,t) = \varphi_>(x)\exp(iqy)\exp(-i\omega t) \tag{26}$$

$$\varphi_>(x) \simeq \frac{2\sigma_{xx}}{i\omega\kappa}\int_0^{+\infty} K_0(|x-s|)\left[\frac{\partial^2\varphi_>}{\partial s^2}+\frac{\partial^2\varphi_<}{\partial s^2}\right]ds, \quad x \geq 0. \tag{27}$$

$K_0(x)$ being the zero order Bessel function of imaginary argument.

To the right of point $x = 0$ the conductivity σ_{xx} in (27) has some small efective value different from its quantum value $\sigma_{xx} = 0$ at an integer shelf. Zero σ_{xx} in the vicinity of $x = 0$ is accounted for by introducing a discontinuity in the potential described by two separate functions $\varphi_>(x,y,t)$ and $\varphi_<(x,y,t)$ appropriately matched at the line $x = x_4 \pm 0$.

To the left of the point $x = x_4 - 0$ (or $x = 0$ for (27)) the 2D electron stripe is squeezed from both sides by zero normal current conditions. This allows one to consider it as effectively quasi-one-dimensional system responding only to the fields depending on the y coordinate,

$$-i\omega\delta n_l(y) + \sigma_{yy}(\omega,H)\left[\frac{\partial^2\varphi_>}{\partial y^2}+\frac{\partial^2\varphi_<}{\partial y^2}\right] \simeq 0, \quad \delta n_l(y,t) \simeq \int_0^{x_4}\delta n_s^<(x,y,t)dx \tag{28}$$

$$\varphi_<(x,y) \simeq e\delta n_l(y)K_0[q(x-a_4)] \tag{29}$$

The potential $\varphi_<(x,y)$ (29) is typical of the quasi-one-dimensional conductors with a logarithmic singularity at the filament axis which is in any case cut off at the length equal to a_4 with a_l taken from (20). As a rough estimate one obtains, assuming in (28) $\varphi_> \sim 0$ and $\sigma_{yy} \propto (i\omega)^{-1}$, that equations (28), (29) contain the dispersion law $\omega \propto q$ typical of one-dimensional conductors. The simplification (28), (29) is not critical. The problem with discontinuity at the line $x = x_4 - 0$ can also be accurately formulated for the case of two boundary conditions of different types. On of them has the same sense as (25). The other condition, classical, preserves the structure of Eq. (2).

The two equations (27), (28) determine the spectrum of EMP-mode along the integer stripe located at x_4 close to the edge of the 2D disk with elliptic profile (7). The outer part of this structure is actually a quasi-one-dimensional ring which partly screens the fields of the EMP-mode localized at the inner side of the integer stripe with the coordinate x_4 in Fig. 3.

To solve this equation set, one can try a perturbation theory since $\varphi_> \propto \sigma_{xy}$ while the perturbation $\varphi_<(x,y) \propto \sigma_{yy}$ (which verified directly) and additionally the inequality

$\sigma_{yy}/\sigma_{xy} \ll 1$ is assumed to be satisfied. In that case the zero approximation to solution of equation set (27), (28) satisfies the integro-differential equations

$$\varphi_>(x) \simeq \frac{2\sigma_{xx}}{i\omega\kappa} \int\limits_0^{+\infty} K_0(|x-s|)\frac{\partial^2\varphi_>}{\partial s^2}ds, \quad x \geq 0, \quad d^2\varphi_>/dx^2 \gg d^2\varphi_>/dy^2 \tag{30}$$

for $\varphi_>(x)$ with the boundary condition

$$\sigma_{xx}\varphi'_>(0) + iq\sigma_{xy}\varphi_>(0) = 0 \tag{31}$$

Integrating Eq. (30) by parts and then adding and subtracting in the r.h.s of the definition of $\varphi_>(x)$ the combinations

$$K_0(qx)\varphi'_>(x) \Longleftrightarrow \int\limits_0^{+\infty} \frac{\partial K_0(q|x-s|)}{\partial s}\varphi'_>(x)ds,$$

one obtains

$$\varphi_>(x) \simeq \frac{2\sigma_{xx}}{i\omega\kappa}\left\{K_0(qx)[\varphi'_>(0) - \varphi'_>(x)] + \int\limits_0^{+\infty} \frac{\partial K_0(q|x-s|)}{\partial s}[\varphi'_>(x) - \varphi'_>(s)]ds, \right\}. \tag{32}$$

Substitution into the expression (32) for $\varphi_>(x)$ of the value $x = 0$ yields

$$\varphi_>(0) = \frac{2\sigma_{xx}}{i\omega\kappa}\varphi'_>(0) \int\limits_0^{+\infty} \left[1 - \frac{\varphi'_>(s)}{\varphi'_>(0)}\right] \frac{\partial K_0(qs)}{\partial s}ds \tag{33}$$

Further analysis of Eq. (33) is based on the hypothesis that

$$\frac{\varphi_>(0)}{\varphi'_>(0)} \simeq -l, \quad \text{and} \quad \left[1 - \frac{\varphi'_>(s)}{\varphi'_>(0)}\right] \simeq \begin{cases} 0, & x < l \\ 1 & x > l. \end{cases} \tag{34}$$

Then equations (34) and (33) yield

$$-l \simeq \frac{2\sigma_{xx}}{i\omega\kappa}K_0(ql). \tag{35}$$

As a consequence, boundary condition (31) together with (34) and (35) result in

$$\omega(q) \simeq \frac{2\sigma_{xy}}{\kappa}qK_0(ql), \quad \omega \ll \omega_c. \tag{36}$$

It is important that the conductivity σ_{xx} in the definition (35) for l has a finite value shown by dashed lines in the vicinity of the edges of the integer stripe in Fig. 3. The

zero value of $\sigma_{xx}(\nu_l) \equiv 0$ itself within the integer stripe is accounted for by the boundary conditions (25), (31).

The dispersion law (36) reveals the existence (just as in Ref. [20]) of a standard EMP-mode along the *integer*-stripe whose axis is positioned at $x = x_4$ on the density profile $n(x)$ in Fig. 3. This stament is consistent with the observed data presented in Fig. 2. Vertical line which marks the threshold for suppression of the low-frequency $AEMP$-mode ω_{11}^s corresponds to the magnetic field where the EMP-mode ω_{01}^- demonstrates quite regular behavior.

4. Summary

Proposed is an interpretation of experimental data [5-7] revealing the existence of $AEMP$-excitations in 2D charged disks with a "soft" profile $n(r)$ of degenerate electron density. The discussion covers asymptotic behavior of such excitations in strong magnetic fields $H \gg H_{max}$ where H_{max} is the field at which a characteristic peak in the $\omega_{ac}(H)$ curve occurs. The analysis is based on the elliptic approximation (7) for electron density profile $n(r)$. The axially symmetric elliptic approximation is shown to much more realistic in calculations of the observed $AEMP$-excitations in 2D disks [5-7] than the usually employed "semi-infinite" approach. Parameter δ (21), which qualitatively measures the ellipticity degree of the problem is, according to data of Ref. [5], ~ 1 (for the semi-infinite geometry ($\subset$-formalism) it should satisfy the inequality $\delta \ll 1$), the observed indices l and m of $AEMP$-excitations in Fig. 2 are close to the minimal possible ones, which also creates difficulties in applying the half-plane formalism [8] to the observed $AEMP$-dynamics with axial symmetry.

An additional argument favoring $AEMP$-origin of the observed modes is a beautiful effect of their suppression in magnetic fields $H > H_{thresh}$ which are high enough for development in the vicinity of the 2D disk boundary of *integer*-stripes typical of QHE. Formally, this results in adding to the equations describing the EMP-excitations one more requirement (25), (31) affecting the EMP-dynamics governed by the boundary condition (2). Analysis of equations (27),(28) accounting for the boundary conditions (2), (31) reveals that in this formulation the $AEMP$-modes do not survive which is confirmed by experiment.

The author is grateful to S.Nazin for very useful discussions, constructive remarks and

help in drawing figures. My acknowledgements are also to I.Andreev, V.Muraviev, and I.Kukushkin for discussion of general situation in $AEMP$-problem and useful remarks.

References

1. S.Nazin, V.Shikin, ZhETF, 94, (1988), 133 (in Russian)

2. S.Nazin, V.Shikin, FNT 15, (1989), 227 (in Russian)

3. E.Elliott, C.Pakes, L.Skrbek and W.Vinen, Phys.Rev.Lett, 75, (1995), 3713

4. E.Elliott, S.Nazin, C.Pakes, L.Skrbek , W.Vinen, G.Cox, Phys.Rev. B 56, (1997), 3447

5. D.Smetnev, V.Muraviev, I.Andreev, I.Kukushkin, Pis'ma ZhETF, 94,(2011), 141 (in Russian)

6. I.Andreev, V.Muravev, I.Kukushkin, Pis'ma ZhETF, 96, (2012), 588 (in Russian)

7. I.Andreev, V.Muravev, D.Smetnev, I.Kukushkin, Phys.Rev B 86, (2012), 125315

8. L.Aleiner, L.Glazman Phys.Rev.Lett, 72, (1994), 2935

9. G.Ernst, R.Haug,, J.Kuhl, K. von Klitzing, K.Eberl, Phys.Rev.Lett 77, (1996), 4245

10. V.Shikin, S.Nazin, ZhETF 113, (2011), 306 (in Russian)

11. S.Nazin and V.Shikin, Quantum Hall effect in narrow Coulomb channels. Physical Review B, 84 (2011) 153301

12. D.Chklovskii, B.Shklovskii, L.Glazman, Phys. Rev. B 46 (1992), 4026.

13. D.Chklovski, K.Matveev, B.Shklovskii, Phys. Rev. B 47, (1993), 12605

14. K.Lier, R.Gerhardts, Phys.Rev. B 50, (1994), 7757

15. J.Oh, R.Gerhardts, Phys.Rev. B 56, (1997) 13519

16. A.Siddiki, R.Gerhardts, Phys.Rev. B 70, (2004), 195335

17. V.Shikin, Yu.Shikina, FTT 39, (1997), 742 (in Russian)

18. V.Shikin, Pis'ma ZhETF, 73, (2001), 283 ; 73, (2001), 605 (in Russian)

19. E.Devyatov, UFN, 177, (2007), 207 (in Russian)

20. A.Mikhailov, in *Horison in World Physics*, edited by O.Kirichek, v.236, Chap.1 (Nova, New York, 2000), p 1-47